FRACTURE OF CONCRETE CYLINDERS SUBJECTED TO TORSION

G. Lilliu and J.G.M. van Mier

Microlab, Faculty of Civil Engineering and Geosciences,
Delft University of Technology
P.O. Box 5048, 2600 GA Delft, The Netherlands

ABSTRACT

In order to validate the 3D version of the 2D 'Delft' lattice model some torsion tests were conducted on concrete cylinders, both notched and un-notched. A biaxial loading machine with rotational and vertical loading axes was used. Tests were conducted under different axial restraints. It was observed that a perturbation of the stress state induced by the torque may affect significantly the crack pattern. Under axial compressive stress, after a spiralling crack, an axial crack was detected in un-notched specimens. In notched cylinders, the failure surface is conical if an axial load is present, while it appears flat and localized within the notch height in case no axial load is applied.

KEYWORDS

Concrete, 3D fracture, torsion, multiaxial stress.

INTRODUCTION

At the beginning of the 1990's a 2D lattice model was developed in Delft [1]. In the past ten years this model has been used for simulating experiments on concrete specimens subjected to plane stress. Despite the realistic crack patterns, the response of the model in terms of load-displacement diagrams has always been far too brittle when compared with the experimental results. A possible cause is that fracture processes are 3D phenomena. In fact, the presence of randomly distributed inclusions in the material (aggregates) produces curvatures of the crack surface in all directions. As a consequence, the dissipated energy increases. For this reason, a 3D version of the lattice model was developed [2] and torsion tests were designed to validate the numerical simulations.

Several attempts have been made in the past to design a set-up for conducting torsion experiments on cylinders [3,4]. The main reason for conducting torsion tests was that they could likely give insight in the mode III fracture energy, G_f^{III}. The same tests, conducted on notched cylinders, allow measurements of mode II fracture energy, G_f^{II}. In notched cylinders the shear stresses induced by the applied torque should produce a planar crack and, as a result, G_f^{III} and G_f^{II} should coincide. However, it seems that the condition of pure shear stress cannot be achieved in practice. There is experimental evidence that shear fracture tests are very sensitive to axial restraints, such as the axial compressive force arising from presence of friction at the supports. In the torsion tests it has been observed that the failure surface can change drastically from planar to conical [5].

by the axial restraint makes torsion tests particularly suitable for validation of the 3D lattice model and other numerical models in general. In this paper an overview is given of the results of torsion tests on concrete. They form the basis for validation of the 3D lattice model.

EXPERIMENTAL DETAILS

Tests were conducted on concrete cylinders with diameter D=34 mm and height H=68 mm. Both un-notched and notched cylinders were used. The notch, at half height of the cylinder, has a depth d_0=8 mm.

The specimens were drilled from concrete blocks, casted in plywood moulds. The aggregates used for the mixture have maximum size d_a=2 mm. Portland CEM I 32.5R cement was used, with water/cement ratio 0.4. During pouring of the mixture and for other 30 seconds after complete filling, the moulds were vibrated on a small vibrating table. Next, they were covered with plastic sheets. After two days, the concrete blocks were demoulded and placed under water. The cylinders, drilled from the concrete blocks after 28 days, were kept in a climate box, at 20^0 temperature and 90% relative humidity, till the moment of testing.

The tests were conducted with a servo-hydraulic INSTRON 8874. This machine has rotational and vertical loading axes, which can be coupled or de-coupled. The maximum loads which can be reached are 100 Nm and 10 kN, respectively. The feed-back signal during the tests is the rotation, measured with a rotational potentiometer connected to a wire attached to the upper loading platen, as shown in Figure 1.

Different tests with different axial restraint were conducted. The cases considered are: zero axial force, zero axial displacement and constant axial compressive force, corresponding to a nominal stress of -4 MPa. An hour before testing the specimen was glued to the loading platens. After hardening of the glue, the axial load was applied first, whereafter the rotational load was applied at the constant speed of 0.002 deg/sec. During the tests the axial displacement (stroke), the axial load, the rotation and the torque were recorded.

Figure 1: Set-up for measurements of the rotational angle

EXPERIMENTAL RESULTS

For each loading condition, three tests were conducted. The average of the peak torque and of the axial load, with the corresponding standard deviations, are reported in Table 1. There, the tests are named after the applied loading condition: d2**f**, d2**d** and d2**c** refer to tests on cylinders without notch under zero axial **f**orce, zero axial **d**isplacement and constant axial **c**ompression, respectively. In the same way, d2nf, d2nd and d2nc refer to tests on notched cylinders. In Figure 2 and Figure 3, some of the obtained experimental results are reported, together with the crack patterns. The torque versus rotation curves are represented with a continuous line, while the stroke (LVDT in the hydraulic actuator) or the axial load (depending if the experiment was conducted under constant load or fixed displacement) are represented with a dashed line. In the insets in the diagrams, the crack patterns are those photographed after the end of the test, when the upper loading platen was driven far from the bottom platen. The other crack patterns shown in these figures were photographed from different orientations

TABLE 1
EXPERIMENTAL RESULTS

	d2f	d2d	d2c	d2nf	d2nd	d2nc
Avr. Torque [Nm]	66.8	70.0(3.3)	93.6(3.3)	24.4(0.8)	51.7(1.7)	49.0(1.0)
Max. Load [kN]	0	-3.5(0.9)	-3.6	0	-4.7(0.2)	-1.1

Average of three test results and standard deviations (between parenthesis). In d2f the average is computed on two test results.

Un-notched cylinders

Independently from the axial restraint, the crack which can be detected as first with the naked eye is that with label 1 in the subfigures of Figure 2. This crack spirals around the specimen. It is not clear if it starts along the body of the specimen or at one of the ends, since it could be detected only after it covered the whole length of the cylinder. According to the solution of the linear elastic problem, the twisting moment is constant and the crack initiation should be just a consequence of stress concentrations due to the internal structure of the material. However, the specimen is clamped to the loading platens and cannot contract freely. As a consequence, a biaxial tensile stress state might arise at the ends of the specimen causing crack initiation. Other cracks, indicated with the label 2, depart from the spiralling crack as ”wings”. The spiralling crack can be either continuous or consists of more overlapping branches, like shown in Figure 2-a_1. In other cases, more than one of such cracks can be detected (see Figure 2-b_1, b_3 and b_4).

When no axial load is applied, the spiralling crack travels towards the end of the specimen (Figure 2-a_4) and turns, forming a loop (Figure 2-a_3). In case of axial restraint, vertical cracks develop, producing spalling of concrete, as shown in Figure 2-c_1. The cases of zero axial displacement (Figure 2, right top diagram) and constant axial compressive load are similar. In fact, when the specimen cannot elongate freely, a compressive force arises. Thus, the vertical cracks seem a consequence of the axial compressive stresses, although these are of very limited magnitude (4 MPa).

The torque-rotation diagrams have a peak and a softening branch. The tests stop when the external rotation has reached the maximum value, namely 10 deg. When there is no axial load the softening branch is extremely smooth and presents a long tail. The shape of the diagrams is somehow more complex when there is an axial restraint. In case of zero axial displacement, the torque-rotation diagram starts to descend gradually when the compressive force has reached the maximum value. Then, it shows changes of curvature, with corresponding changes of slope in the load-rotation curve. In case of compressive load, as in case of zero axial load, the diagram drops after the peak and the post-peak region is characterized by several changes of curvature, corresponding to a small elongation of the specimen. Afterwards, the cylinder begins to contract and the torque increases with the rotation. The presence of a constant compressive load seems to be a very effective confinement and, thus, strengthens the material. In fact, the peak torque is much higher than in the case of zero axial displacement, where the compression varies during the test.

Notched cylinders

If no axial restraint is applied, the notch causes the localization of the fracture within its height. During the test, it was possible to observe inclined, parallel cracks on the surface of the cylinder’s core. Coalescence of such cracks produced the final failure, as shown in the inset of the torque-rotation diagram (Figure 3).

When an axial restraint is applied cracking also starts at the notch. However, cracks are not localized within the height of the notch, but develop along half or even the complete specimen length. These cracks are similar to the spiralling cracks observed in the un-notched cylinders and seem to start right at the notch, where they show a wider opening. In the tests conducted under constant axial load only one half of the cylinder, namely the top half, was cracked (see Figure 3-b_1, b_2, b_3 and b_4). Two of the tests conducted under zero axial displacement

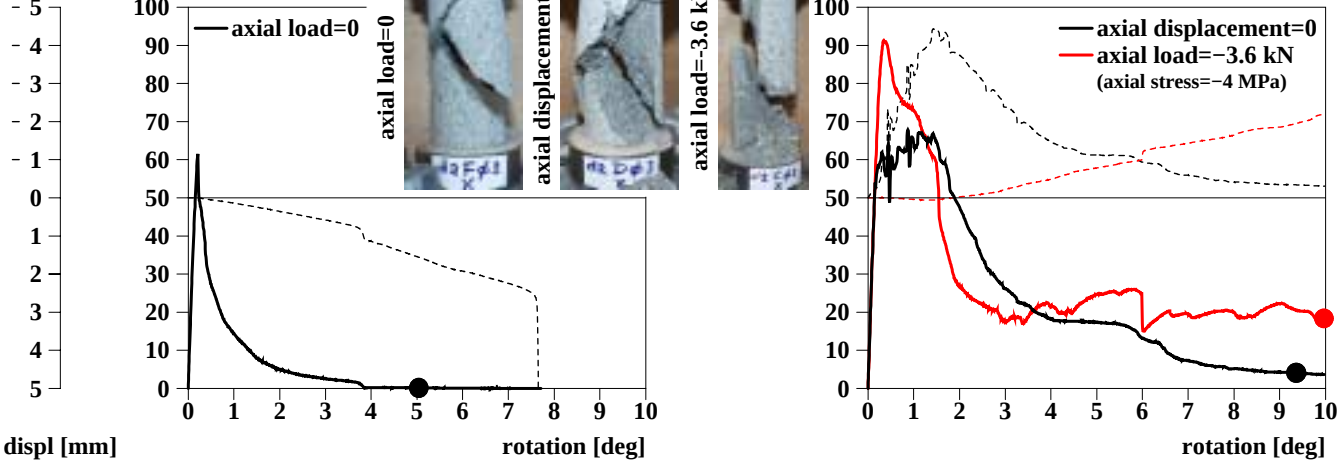

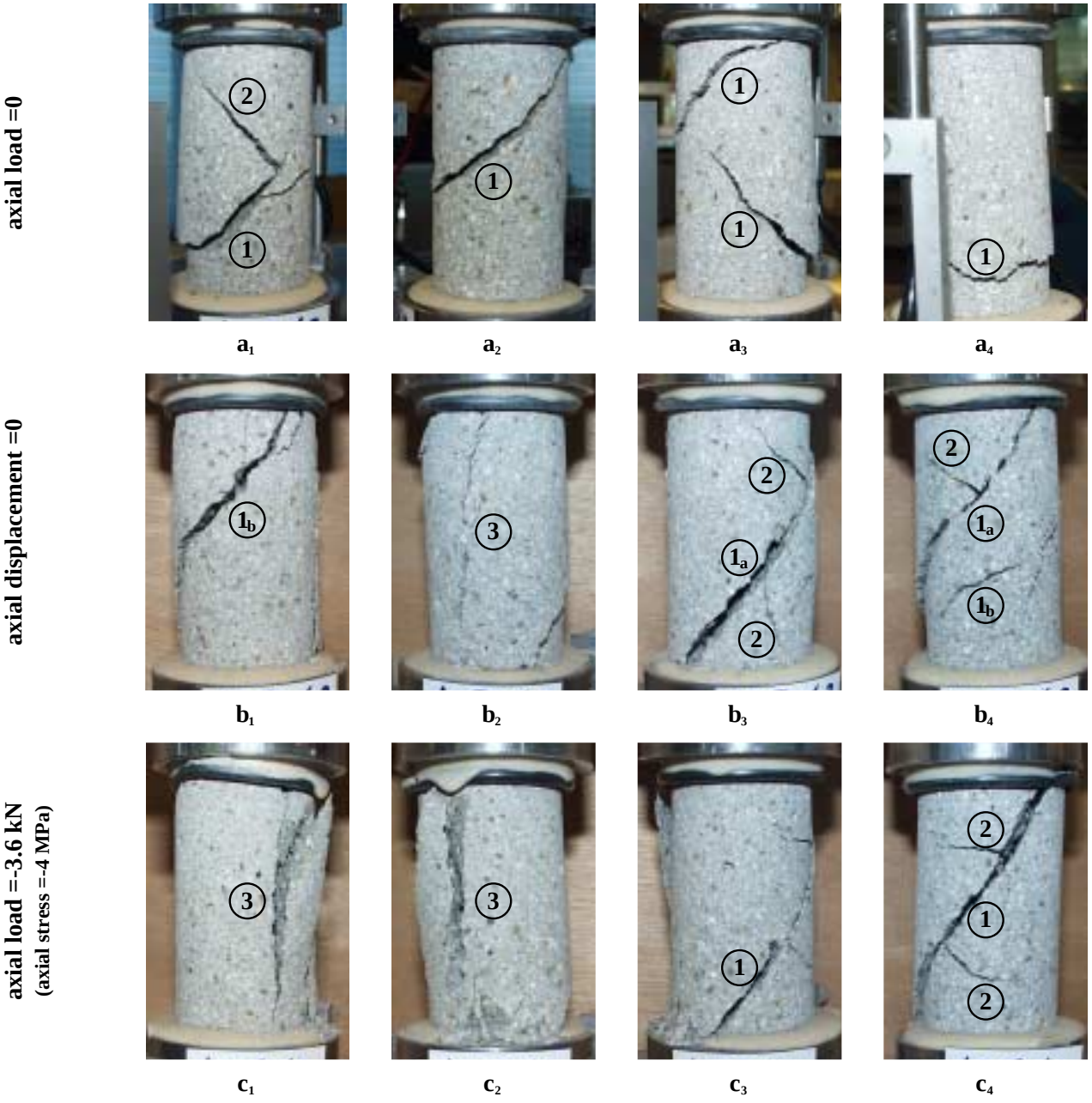

Figure 2: Experimental results obtained with un-notched specimens under zero axial force (a), zero axial displacement (b) and constant compressive load (c)

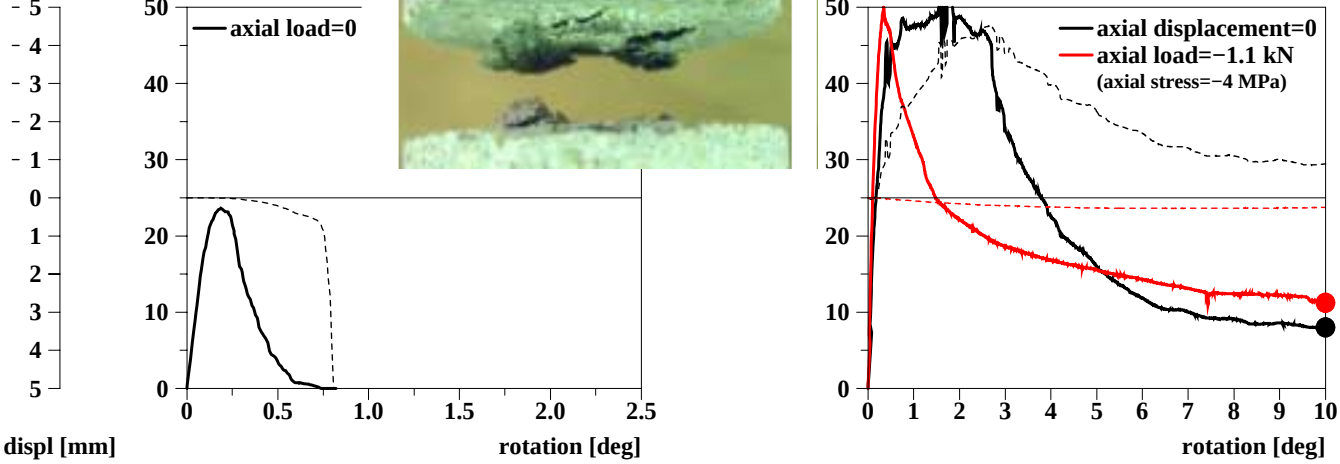

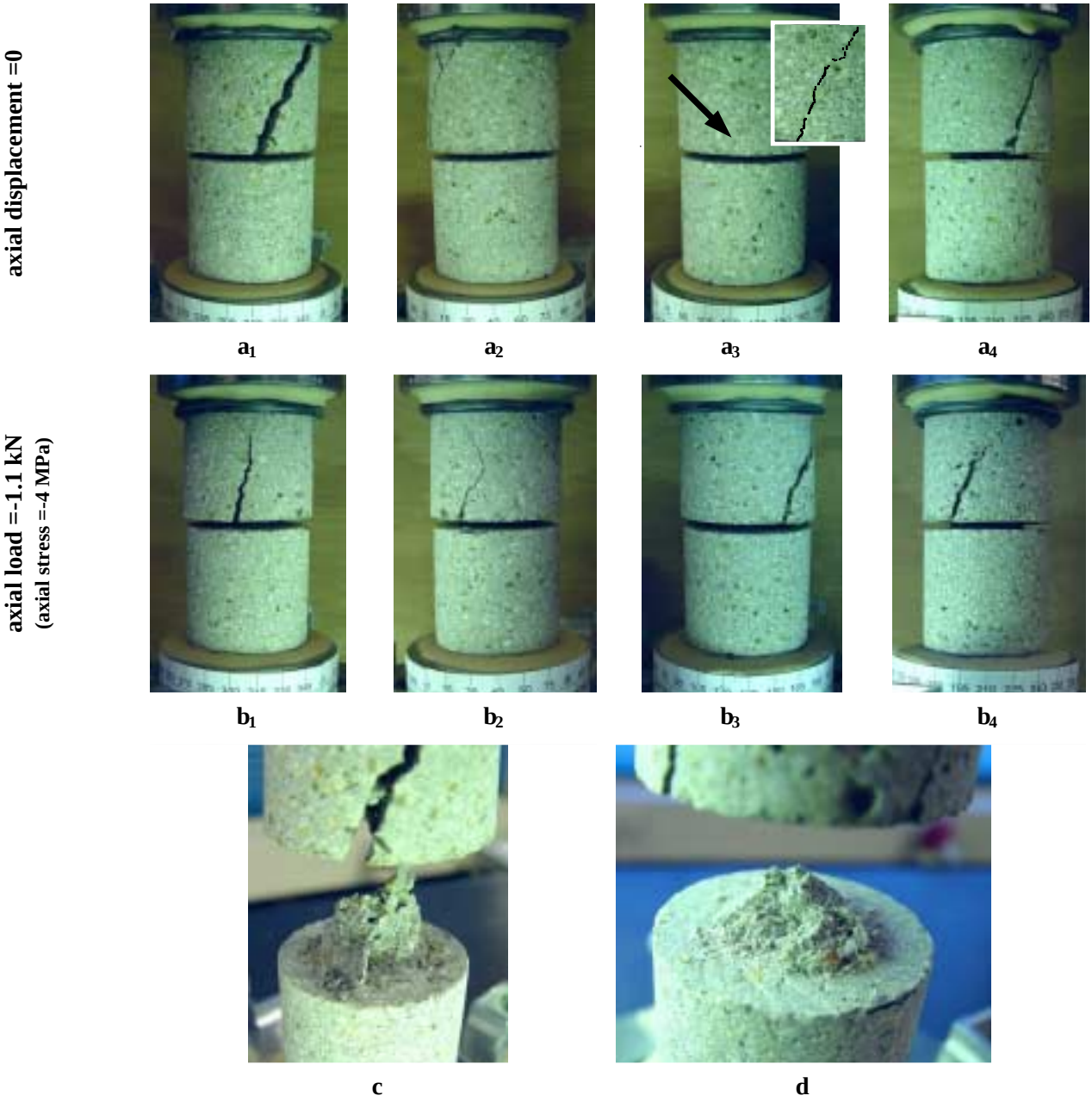

Figure 3: Experimental results obtained with notched specimens under zero axial displacement (a,c) and constant compressive load (b,d)

Figure 3-a_1, a_2, a_3 and a_4). In all the cases considered, a final conical failure surface as reported earlier by Bažant et al. [5] was observed. The cone appeared flatter in the tests conducted under constant compressive force (see Figure 3-d) than in tests under zero axial displacement (see Figure 3-c).

Similar to the tests on un-notched cylinders, in the notched cylinder tests under zero axial displacement a compressive axial force developed. The ascending and descending branch in the load-rotation diagram correspond to an extended zone of nonlinearity and to the softening branch, respectively, in the torque-rotation diagram. The diagrams do not present any change in curvature in the softening branch, as it was observed in the tests on un-notched cylinders. The same happens when the tests are conducted applying a constant compressive force: the torque after the peak decreases gradually without showing changes in curvature. In contrast to the un-notched cylinders, the peak load does not increase when the compressive force is constant during the complete test.

CONCLUSIONS

Torsion tests have been conducted on un-notched and notched concrete cylinders with diameter D=34 mm and height H=68 mm. Different axial restraints were used, namely: zero axial load, zero axial displacement and constant compressive load. The last two loading conditions are somehow similar, since the constrained axial displacement produces as effect a variable axial compression. The crack pattern varies with the adopted axial restraint. In un-notched cylinders the first to develop is a spiralling crack, from which other ”wing” cracks may depart. Vertical cracks appear if a compressive axial stress is applied. Localized failure within the notch height occurs in notched cylinders or a conical crack surface develops depending on the presence of an axial compressive stress. Like the crack pattern, the torque-rotation diagrams differ with axial constraint. In the tests on un-notched cylinders the presence of an axial compressive load produces changes in curvature of the softening branch and, even, a new final increase of torque. No change of curvature was observed in the same kind of tests conducted on notched cylinders. However, in the case of constrained axial displacement the diagram presents an extended zone surrounding the peak where the torque is practically constant. In all cases considered the sensitivity of torsion tests to the presence of an axial stress is confirmed, eventhough only a small amount of constraint is applied. Because of the chosen geometry and the complexity of the final crack pattern, it is difficult at this stage to give an interpretation of the possible fracture mechanism during loading. Currently it is tried to detect propagation of cracks at different loading stages by means of an impregnation technique.

AKNOWLEDGEMENTS

This research has been made possible through a grant from the Priority Programme Materials Research (PPM) and the Dutch Technology Foundation (STW), which is gratefully aknowledged. The authors are indebted to Mr. G. Timmers for his expert help in designing and performing the experiments.

REFERENCES

1. Schlangen, E. and van Mier, J.G.M. (1992) *Cement and Concrete Composites* 14, pp. 105-118.
2. Lilliu, G. and van Mier J.G.M (2000). In: *Proceedings Materials Week*, Münich, Germany.
3. Yacoub-Tokatly, Z., Barr, B. and Norris, P. (1989). In: *Fracture of Concrete and Rock: Recent Developments*, pp. 596-604, Shah, S.P., Swartz, S.E. and Barr, B. (Eds). Elsevier, New York.
4. Xu Daoyuan and Reinhardt, H.W. (1989). In: *Fracture of Concrete and Rock: Recent Developments*, pp. 39-50, Shah, S.P., Swartz, S.E. and Barr, B. (Eds). Elsevier, New York.
5. Bažant, Z.P., Prat, P.C. and Tabbara, M.R. (1990) *ACI Materials Journal* 87, pp. 12-19.